

# Late Holocene relative sea-level changes in Lebanon, Eastern Mediterranean<sup>☆</sup>

Christophe Morhange<sup>a</sup>, Paolo A. Pirazzoli<sup>b</sup>, Nick Marriner<sup>a,\*</sup>,  
Lucien F. Montaggioni<sup>c</sup>, Tanios Nammour<sup>d</sup>

<sup>a</sup> CNRS-CEREGE, UMR 6635, B.P. 80, Europôle de l'Arbois, F 13545 Aix-en-Provence, Cedex 4, France

<sup>b</sup> CNRS-Laboratoire de Géographie Physique, UMR 8591, F 92195 Meudon Cedex, France

<sup>c</sup> CNRS-FRE 2761, Département des Sciences de la Terre et de l'Environnement, Université de Provence,  
F 13331 Marseille, Cedex 3, France

<sup>d</sup> Université Libanaise, Département de géographie, Beirut, Lebanon

Received 18 November 2005; received in revised form 6 March 2006; accepted 9 April 2006

## Abstract

Twenty-nine <sup>14</sup>C dates of precise biological sea-level indicators from the Lebanese coast show evidence for two significant regional crustal uplift episodes during the past 6000 years. We elucidate: (1) an upper shoreline at ca. +120 to +140 cm, which lasted from ca. 6000 to 3000 BP; and (2) a lower shoreline at +80 ±40 cm, developed between the fifth century BC and the sixth century AD. These movements are associated with: (1) two major seismic crises along the Yammuneh fault and the Roum-Tripoli Thrust (RTT); and (2) subsequent seismic events on a series of second-order ENE trending dextral transpressive faults. Vertical movements affected north Lebanon, whilst the coasts of south Lebanon generally underwent crustal downlift. This is in contrast with relative stability in northern Israel, suggesting an area of stationary tectonic conditions west of the Dead Sea–Rosh Hanikra/Ras Nakoura fault. The main <sup>14</sup>C age cluster, corresponding to the second uplift event, may have resulted from fault movements during the “Early Byzantine Tectonic Paroxysm” (EBTP), between ca. 1750 and 2000 BP. Relative sea level stabilised to present level around 1000 BP.

© 2006 Elsevier B.V. All rights reserved.

*Keywords:* Lebanon; relative sea level; Holocene; geomorphology; tectonics; bioconstruction; Mediterranean

## 1. Introduction

The most active tectonic structure along the eastern shore of the Mediterranean is the north–south trending left-lateral Levant fault system, the plate boundary

between Arabia and Africa. In Lebanon, it forms a 160 km restraining bend responsible for the uplift of Mount Lebanon (Daëron et al., 2004). The study of relative sea-level mobility can provide quantitative constraints for crustal deformation along the Lebanese coast Dead Sea Transform Fault and more particularly the role of the Roum-Tripoli Thrust (RTT). The coast of Lebanon is characterized by well-developed uplifted subtidal bioconstructions e.g. *Dendropoma petraeum*. Our new data allow us to: (1) test the Early Byzantine Tectonic Paroxysm (EBTP) hypothesis (Pirazzoli,

<sup>☆</sup> Dedicated to the memory of Ziad R. Beydoun, Middle East geologist.

\* Corresponding author.

E-mail addresses: morhange@cerge.fr (C. Morhange), pirazzol@cnsr-belleuve.fr (P.A. Pirazzoli), nick.marriner@wanadoo.fr (N. Marriner), lmontag@up.univ-mrs.fr (L.F. Montaggioni).

1986a,b; Pirazzoli et al., 1996); and (2) interpret relative sea-level changes in terms of crustal deformation notably the roles of the Roum, Yammuneh and Serghaya faults in connection with the RTT.

Over the past three decades, studies of marks left by former sea levels have shown that numerous vertical displacements took place in the Eastern Mediterranean between ca. 1750 and 2000 BP. After calibration, the period concerned ranges from the mid-4th century to mid-6th century AD. Field results from the islands of Crete and Antikythira, and data compilation from other areas, suggested that these movements could be correlated (Pirazzoli, 1986a,b). This tectonic episode was called the EBTP. Later, these vertical displacements were further documented along the coasts of Hatay (Pirazzoli et al., 1991), Syria (Dalongeville et al., 1993), the Ionian Islands (Pirazzoli et al., 1994a), and the Gulf of Corinth (Pirazzoli et al., 1994b). Further evidence for the EBTP has been reported from the Gulf of Corinth (Stiros and Pirazzoli, 1998), possibly Samos Island (Stiros et al., 2000), and Tripolitana (Di Vita, 1990).

Elevated fossil benches along the Lebanese coast, mainly between Tripoli and Beirut, were first reported 40 years ago and ascribed to historical tectonic movements (Fevret and Sanlaville, 1965, 1966). These features were reinterpreted as elevated eustatic shorelines, lasting from the 2nd century BC to the 2nd or 3rd centuries AD, and called the “Tabarjan” (Sanlaville, 1970, 1977). This interpretation was challenged by Pirazzoli (1976) and interpreted as possible evidence for the EBTP along the Lebanese coast.

## 2. Seismotectonic setting

Lebanon coincides with a restraining bend of the left-lateral Dead Sea fault system that marks the transform boundary between the African and Arabian plates (Fig. 1). The fault system, which stretches from the Gulf of Aqaba in the south up to the East Anatolian fault in the north, has propagated across the Levantine regions since the early Pliocene (Garfunkel, 1981). The restraining bend of the transform fault system, which controls the first-order topography of the mountainous areas of Lebanon and Syria, is not confined to a simple fault trace (Fig. 2). It is a fan-shaped fault system resulting from the split of the Dead Sea fault north of the Hula pull-apart in northern Israel (Zilberman et al., 2000), into three main splay faults that are, from west to east, the Roum, Yammuneh and Serghaya faults (Walley, 1988, 1998). Recent research suggests that the RTT might

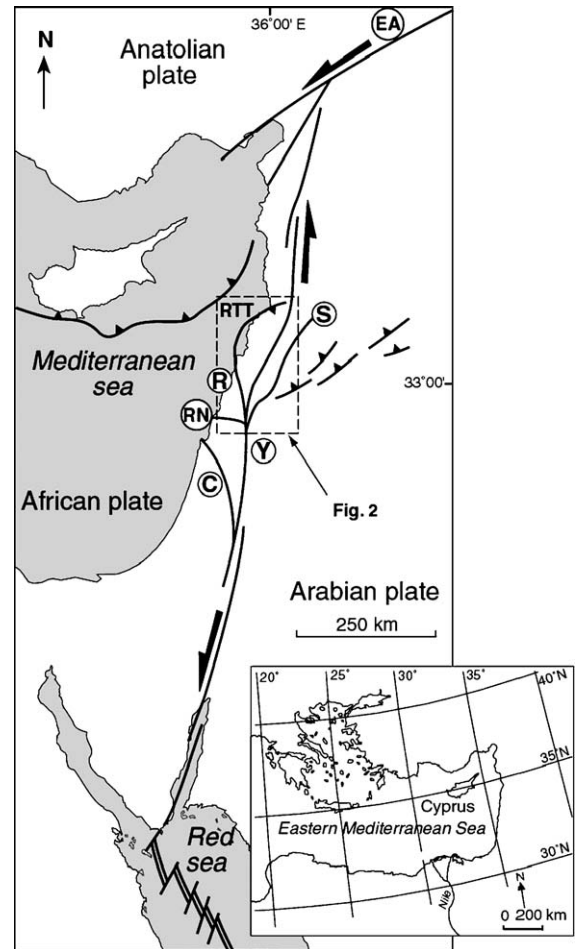


Fig. 1. Tectonic setting of the Lebanese portion of the Dead Sea Transform fault system. C — Carmel fault; R — Roum fault; Y — Yammuneh fault; S — Serghaya fault; RN — Rosh Hanikra/Ras Nakoura fault, EA — East Anatolian fault.

correspond to an offshore thrust system linking the Roum fault and the Tripoli thrust (Elias et al., 2003; Daëron et al., 2005).

Strong and repeated historical earthquakes occurred in the Levantine regions (Kallner-Amiran, 1950; Plassard and Kogoj, 1981; Guidoboni et al., 1994; Mart and Percman, 1996) but none of these events has been linked to any kinematics nor fault segments in Lebanon. Recent palaeoseismological investigations indicate a high level of activity on the Yammuneh and Serghaya faults throughout the Holocene with repeated  $M=7$  events and a high level of seismic hazard along the Yammuneh fault that cuts across the entire restraining bend (Gomez et al., 2003; Daëron et al., 2005). Preliminary cosmogenic dating of offset fans along the Yammuneh fault indicates an integrated slip rate of 5–10 mm/yr over the past 8000 years (Daëron et al., 2004),

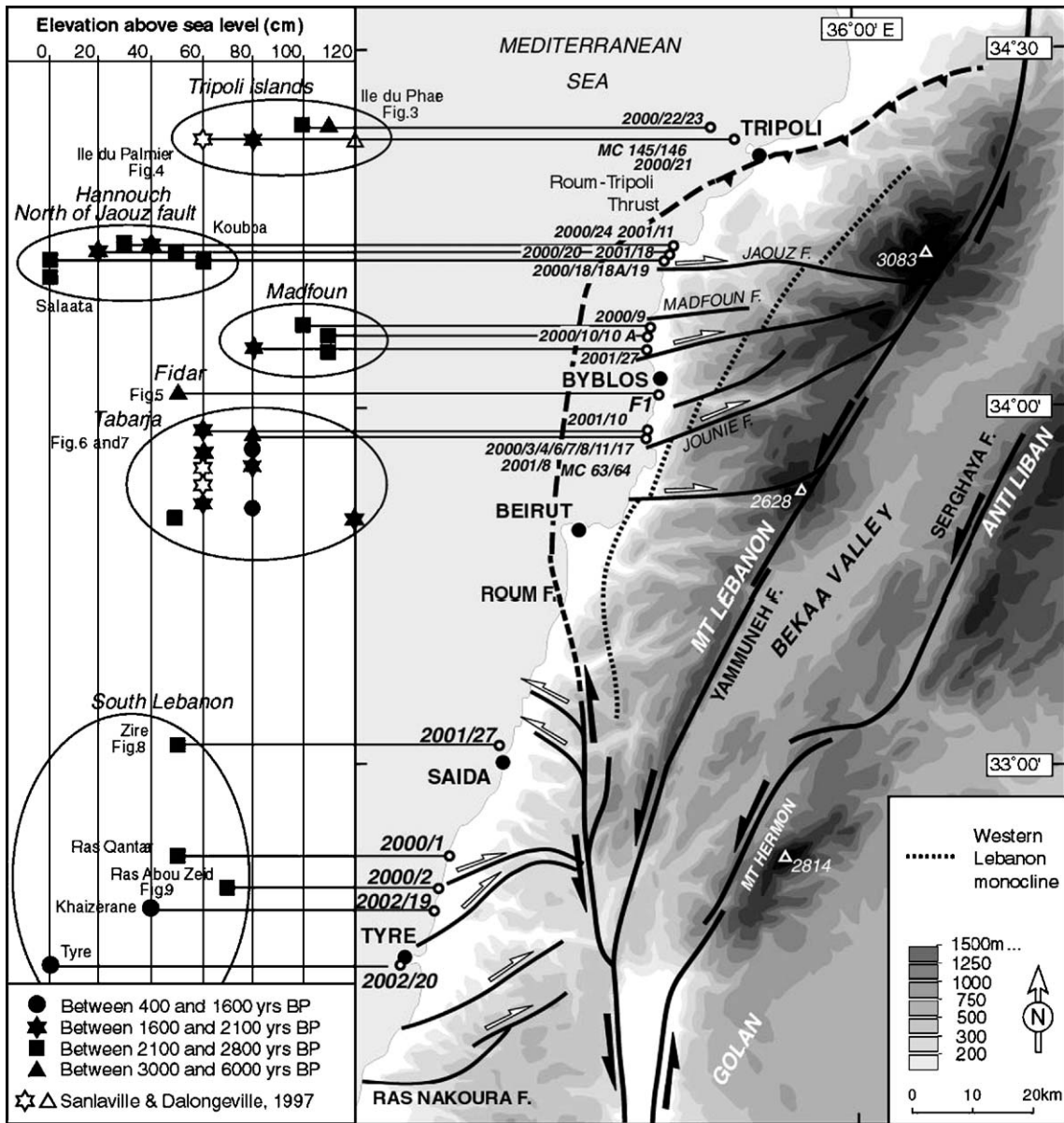


Fig. 2. Structural map of Lebanon and adjacent areas. Sample locations and their corresponding elevation above sea level are shown on the left-hand side of the figure.

whilst the late Holocene slip rate along the Missyaf segment (i.e. the northern extension of the fault in Syria) is estimated to be around 7 mm/yr (Meghraoui et al., 2003). This palaeoseismic estimate appears, however, to be quite high with respect to the integrated late Pleistocene slip rate of 4 mm/yr deduced from offset geomorphic features along the transform south of the Lebanese splay (Klinger et al., 2000). Despite its seismogenic character, the seismic behavior and Holocene slip rate of the Roum fault are not constrained. Yet,

based on geomorphic arguments, the fault is considered to be a particularly active segment of the Levantine restraining bend (Butler et al., 1998; Khair, 2001).

Most of the late Holocene palaeo-shorelines exposed north of Beirut are found on rocky shorelines of a crustal panel, the Mount Lebanon block, bounded to the south by the Roum fault, to the east by the Yammuneh fault and to the north and north-west by the RTT. The most prominent structural feature of this panel is the monocline that runs almost parallel to the coast and

the series of WSW–ENE to E–W trending faults showing a dominant finite right-lateral component of slip (Dubertret, 1955; Dubertret, 1975; Beydoun, 1977; Walley, 1998; Fig. 2). Palaeo-shorelines found south of Beirut belong to a slightly lower-elevation panel, called hereafter the Tyre–Saida block, bounded to the east by the Roum fault and to the south by the Rosh Hanikra–Ras Nakoura fault (Fig. 2). The internal fan-shaped fault pattern of this panel is characterised by dominantly NW trending dextral faults to the south and dominantly WNW trending sinistral faults to the north slip (Ron et al., 1984; Ron and Eyal, 1985).

### 3. Methods

Fossil biological and geomorphological indicators have been used to identify and estimate former sea-level positions (see Laborel and Laborel-Deguen, 1994 for detailed discussion). The limit between the midlittoral and subtidal zones is marked by a sudden increase in species diversity, which corresponds to biological sea level. This benchmark, which incorporates tidal variations and wave exposure, appears as a line between the lower cupulae of midlittoral limpet erosion and the subtidal bioconstructions (e.g., a vermetid rim). Bioconstructions, on the outer edge of the abrasion platform, are built by the close association of two species: the vermetid gastropod *D. petraeum* and the coralline alga *Neogoniolithon notarisii* (Lipkin and Safriel, 1971; Safriel, 1975; Tzur and Safriel, 1978; Barash and Zenziper, 1985). Thus, the upper surface of *Dendropoma* rims precisely marks the upper limit of the subtidal zone (Laborel and Laborel-Deguen, 1994). They are accurate markers of mean sea level. When colonies of elevated in situ *Dendropoma* rims were found capping the rock, their flat upper surface was used as a fossil sea-level indicator (accuracy of  $\pm 10$  cm to  $\pm 20$  cm). The lower limit of the bioconstructions is much less constant relative to wave exposure. The present vertical range of the living species varies from 10 cm in sheltered areas to 40 cm, sometimes more, at exposed sites. The accuracy and precision of the upper limit of this indicator are therefore appropriate for estimating the elevation of uplifted remains.

Marine calcareous alga develop in the infralittoral zone and their upper extension therefore indicates a minimum biological sea-level position. Tidal notches are often good morphological sea-level indicators, with an accuracy up to  $\pm 10$  cm (Pirazzoli, 1986a,b). Spring tidal range is less than 45 cm.

Samples were cut using a diamond saw and the section checked under stereomicroscope. The vermetid

tubes comprised aragonite, with biologically altered parts being chiseled away. The material was  $^{14}\text{C}$  dated at the Laboratoire de Géochronologie de Lyon, and the Poznan and Groningen AMS laboratories. Radiocarbon dates from marine specimens have been conventionally corrected using  $^{13}\text{C}$  measurements and later calibrated (Stuiver et al., 1998a,b). Calibrated dates are quoted to  $2\sigma$ .

### 4. Sea-level data

The sites investigated are presented from north to south. Radiocarbon data are given in Table 1 and sample locations are indicated on Fig. 2.

#### 4.1. Ile du Phare (Ramkine island, Tripoli)

On the southwestern cliffs of the island, two elevated notches undercutting the Miocene substratum have been measured at ca. +120 cm and +140 cm above present biological mean sea level (Fig. 3A). At the same location, the outer part of a calcareous algal crust and associated *Dendropoma* construction collected at +100 cm (sample LIB 2000-23) yielded an age of  $2630 \pm 35$  BP. On the wall of an indentation, marks of a double organic cornice were measured at ca. +100 cm and +140 cm respectively (Fig. 3B), but the upper outcrop could not be reached for sampling. The two cornices clearly indicate, with an uncertainty range of ca.  $\pm 20$  cm, the position of two former biological sea levels.

On the northern coast of the island, a double elevated bench exists at +90 cm and +120 cm, respectively. A *Dendropoma* sample (LIB 2000-22), collected at ca. +110 cm from the base of the notch delimiting the upper bench, yielded a much older age:  $5975 \pm 40$  BP.

#### 4.2. Ile du Palmier (Tripoli)

A date of  $1880 \pm 50$  BP (MC-146) was previously reported for a sample of vermetids bordering an elevated bench at ca. +60 cm, and another date of  $3490 \pm 80$  BP (MC-145) for a crust of unidentified vermetids, sampled at +220 cm from a rock fissure on the northern shore of the island (Sanlaville et al., 1997).

On the northern shore of the island, well-preserved colonies of *Dendropoma* are found at ca. +80 cm (Fig. 4). Sample (LIB 2000-21) was dated  $1810 \pm 35$  BP.

#### 4.3. Hannouch

Near the promontory of Ras Chekka, a *Dendropoma* sample (LIB 2000-24) collected from an elevated bench



Table 1  
<sup>14</sup>C ages of uplifted marine organisms from the Lebanese coast

Material	Elevation (cm)	<sup>14</sup> C (BP)	σ <sup>13</sup> C (‰)	Cal. BC/AD	Lab. ref.	Field ref.	Lat. N	Long. E
<i>Dendropoma petraeum</i>	100±20	<b>2630±35</b>	3.36	403–265 BC	Ly 10447	LIB 2000-23	34°29.80'	35°45.63'
<i>Dendropoma petraeum</i>	110±20	<b>5975±40</b>	0.94	4514–4339 BC	Lyon 1467 (GrA 18402)	LIB 2000-22	~34°30'	~35°45'
* <i>Vermetus</i> sp.	60	<b>1880±50</b>	est. 0	427–651 AD	MC 146		~34°29'	~35°46'
* <i>Vermetus</i> sp.	220 (?)	<b>3490±80</b>	est. 0	1596–1220 BC	MC 145		~34°29'	~35°46'
<i>Dendropoma petraeum</i>	80±10	<b>1810±35</b>	3.39	548–676 AD	Ly 10446	LIB 2000-21	34°29.75'	35°46.45'
<i>Dendropoma petraeum</i>	35±15	<b>2195±30</b>	3.48	96–253 AD	Ly 10448	LIB 2000-24	~34°18'	~35°40'
<i>Vermetus gigas</i>	40±15	<b>1930±25</b>	Est. 0	410–550 AD	Lyon 2090 (Poz)	LIB 2001-11	34°17.86'	35°40.21'
<i>Vermetus</i> sp.	20±15	<b>2075±35</b>	2.77	235–414 AD	Ly 10445	LIB 2000-20	34°17.08'	35°39.62'
<i>Dendropoma petraeum</i>	50±10	<b>2615±25</b>	0.75	400–250 BC	Lyon 2091 (Poz)	LIB 2001-18	34°17.08'	35°39.62'
<i>Dendropoma petraeum</i>	60±15	<b>2585±35</b>	2.48	375–191 BC	Ly 10444	LIB 2000-19	34°17.02'	35°39.52'
<i>Dendropoma petraeum</i>	0±15	<b>2750±35</b>	0.07	631–387 BC	Ly 10443	LIB 2000-18	34°17.02'	35°39.52'
<i>Dendropoma petraeum</i>	0±15	<b>2600±30</b>	0.35	381–214 BC	Ly 11580	LIB 2000-18A	34°17.02'	35°39.52'
<i>Dendropoma petraeum</i>	100±10	<b>2485±35</b>	0.99	270–70 BC	Ly 10439	LIB 2000-9	34°12.59'	35°38.84'
<i>Dendropoma petraeum</i>	110±10	<b>2340±30</b>	2.12	62 BC–85 AD	Ly 10440	LIB 2000-10	34°12.48'	35°38.60'
<i>Dendropoma petraeum</i>	110±10	<b>2410±45</b>	1.02	180 BC–34 AD	Ly 11576	LIB 2000-10A	34°12.48'	35°38.60'
<i>Dendropoma petraeum</i>	80±10	<b>1995±25</b>	0.33	320–460 AD	Lyon 2092 (Poz)	LIB 2001-27	34°12.12'	35°38.23'
<i>Dendropoma petraeum</i>	50±10	<b>3020±35</b>	0.25	896–776 BC	Ly 9832	F1	34°05.73'	35°39.06'
<i>Vermetus</i> sp.	60±10	<b>2065±40</b>	0.4	237–429 AD	Ly 11575	LIB 2001-10	34°03.28'	35°38.24'
<i>Neogoniolithon notarisi</i>	80±10	<b>3195±35</b>	3.19	1127–922 BC	Ly 10442	LIB 2000-17	34°02.99'	35°38.05'
<i>Balanus</i> sp.	80±10	<b>1160±30</b>	2.64	1207–1302 AD	Lyon 1468 (GrA 18404)	LIB 2000-11	34°02.72'	35°37.83'
<i>Dendropoma petraeum</i>	60±10	<b>1960±35</b>	1.54	380–548 AD	Ly 10386	LIB 2000-3	34°02.11'	35°35.51'
<i>Dendropoma petraeum</i>	80±10	<b>1975±45</b>	2.32	328–550 AD	Ly 10438	LIB 2000-8	~34°02'	~35°35'
* <i>Vermetus</i> sp.	60	<b>2035±130</b>	est. 0	65–563 AD	MC 63		34°02'	35°37'
* <i>Vermetus</i> sp.	60	<b>1960±40</b>	Est. 0	363–555 AD	MC 64		34°02'	35°37'
<i>Dendropoma petraeum</i>	60±10	<b>1970±35</b>	2.61	364–533 AD	Ly 10437	LIB 2000-7	34°01.60'	35°37.36'
<i>Dendropoma petraeum</i>	80±10	<b>1585±35</b>	1.47	729–906 AD	Ly 10387	LIB 2000-4	34°01.74'	35°37.41'
Algal crust	50±10	<b>2220±35</b>	2.62	64–240 AD	Ly 10388	LIB 2000-6	34°01.62'	35°37.38'
<i>Dendropoma petraeum</i>	120±10	<b>1805±30</b>	2.32	560–676 AD	Ly 11574	LIB 2001-8	34°01.45'	35°37.33'
<i>Pirenella conica</i>	50±20	<b>2210±50</b>	Est. 0	46–267 AD	Lyon 2007 (GrA 22126)	LIB 2001-27	33°34.39'	35°22.08'
<i>Vermetus triqueter</i>	50±20	<b>2230±35</b>	0.36	58–230 AD	Lyon 1466 (GrA 18401)	LIB 2000-1	33°27.82'	35°17.59'
<i>Vermetus triqueter</i>	70±20	<b>2525±35</b>	1.18	341–135 BC	Ly 10385	LIB 2000-2	33°23.93'	35°15.45'
<i>Dendropoma petraeum</i>	40±10	<b>1095±30</b>	1.45	1259–1341 AD	Ly 11947	LIB 2002-19	~33°23'	~35°16'
<i>Dendropoma petraeum</i>	0±5	<b>450±50</b>	0	Modern	Ly 11948	LIB 2002-20	~33°16'	~35°10'

\* denotes data from Sanlaville et al. (1997). All other dates are new. See Fig. 2 for locations.

at ca. +35±15 cm yielded an age of 2195±30 BP. A sample of *Vermetus gigas* collected nearby at +40±15 cm (LIB 2001-11) was dated 1930±25 BP.

#### 4.4. Ras Koumba–Salaata harbour

A network of micro-creeks has cut into the Miocene limestone formations north of Ras Koumba. The creek floor, submerged by shallow seawater, is bound by a slightly emerged, irregular fringing bench. A vermetid sample (LIB 2000-20), collected in growth position at

ca. +20±15 cm on the bench, yielded an age of 2075±35 BP. Another sample of *Dendropoma*, from the bench at 50±10 cm (LIB 2001-18), was dated 2615±25 BP.

The jetties of Salaata's new harbour have modified the surrounding area's exposure to wave action, causing a recent local drop of biological sea level by around 30 cm relative to the wave exposure existing prior to harbour construction. In the harbour, two stepped bioconstructions are visible at ca. +30 cm (or present level factoring in the wave exposure

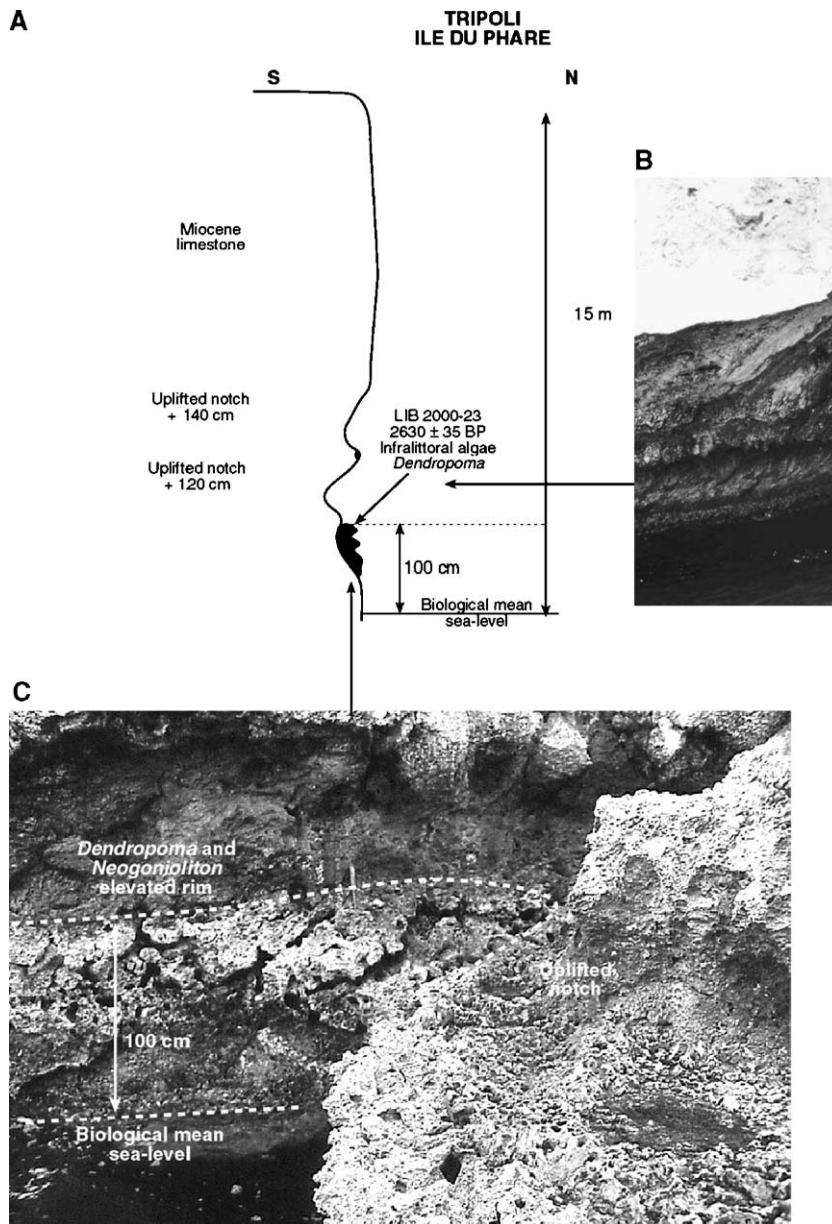


Fig. 3. Location of sea-level biological marker LIB 2000-23 sampled on the Ile du Phare (Tripoli). A double stepped biological bioconstruction has been preserved on the walls of a rock fissure, at ca. +1.0 and +1.3 m, respectively. They could not be reached for sampling, but the lower bioconstruction can be related to remnants of a very close shoreline dated about 2630 BP. The upper bioconstruction can be related to remnants of a shoreline dated ca. 5975 BP on the northern part of the island.

component) and +90 cm (+60 cm) respectively. A *Dendropoma* sample (LIB 2000-19) collected from the upper rim yielded an age of  $2585 \pm 35$  BP. Two other *Dendropoma* samples (LIB 2000-18 and LIB 2000-18A), from the lower rim were dated  $2750 \pm 35$  BP and  $2600 \pm 30$  BP. These data demonstrate that at exposed sites with a favourable bedrock morphology, *Dendropoma* may simultaneously colonise the swash zone, 60 cm apart.

#### 4.5. Ras Madfoun

South of the Madfoun fault (Fig. 2), erosion benches ending in notch profiles at ca. +100 cm, cut the Turonian limestones. A sample of juvenile *Dendropoma* (LIB 2000-9) collected at ca. +100 cm from the base of a mushroom-rock notch yielded an age of  $2485 \pm 35$  BP. Other *Dendropoma* (LIB 2000-10), developed at ca. +110 cm on the outer rim of a bench, gave an age of

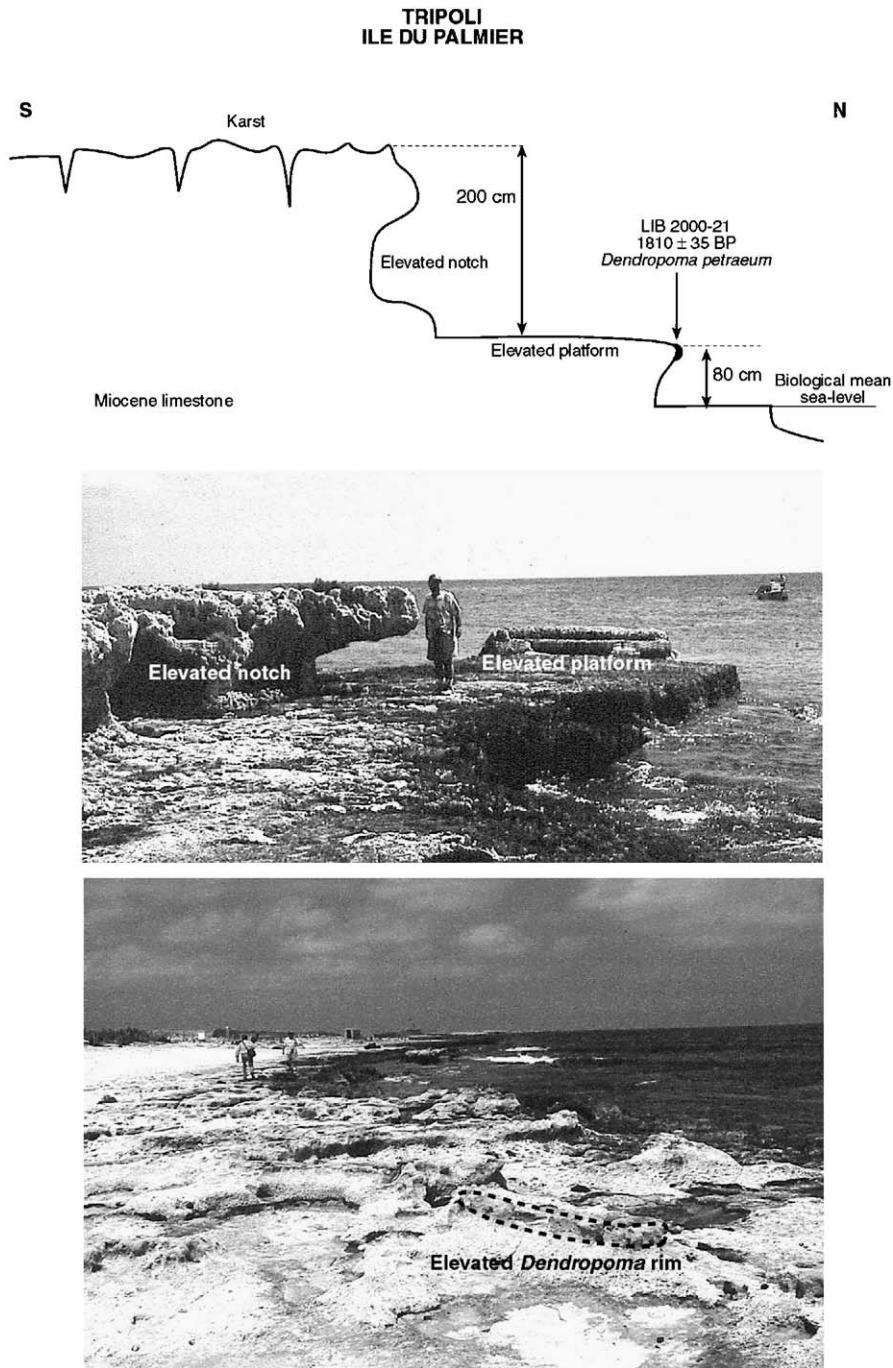


Fig. 4. Location of sea-level biological marker LIB 2000-21 sampled on the Ile du Palmier (Tripoli) and corresponding photograph.

2340±30 BP. A different sample from this same colony (LIB 2000-10A) yielded an age of 2410±45 BP.

Further south of the Madfoun fault (ca. 1 km from sample LIB 2000-10), biological remains show lower elevations. A *Dendropoma* sample at 80±10 cm (LIB 2001-27) has been AMS dated to 1995±25 BP.

#### 4.6. Fidar creek

North of the southern Fidar creek (Fig. 5), a limestone bench is capped on its outer edge by a *Dendropoma* rim and partially covered by beach-rock. A *Dendropoma* sample (F1) at 50±10 cm, collected



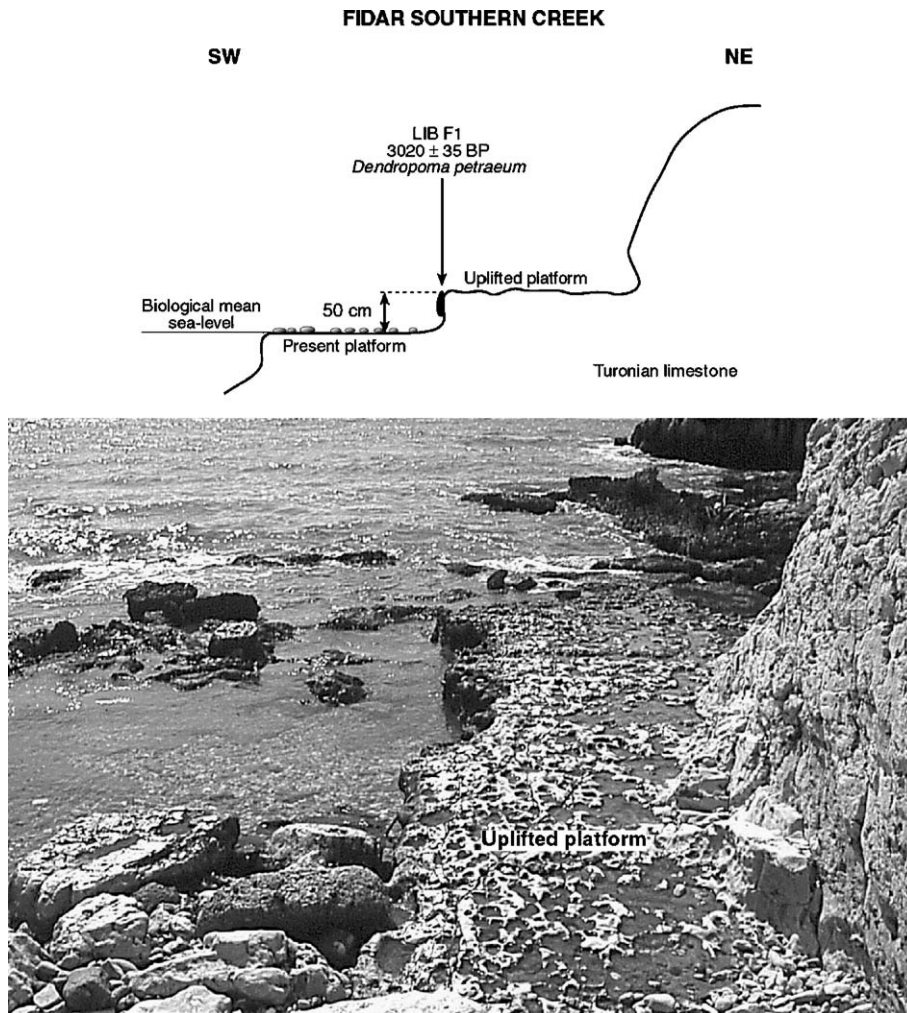


Fig. 5. Schematic section of the sample F1 collected near southern Fidar creek and corresponding photograph.

from the rim, was dated  $3020 \pm 35$  BP. This 'old' date results from the death of the molluscs by sediment overlapping, prior to any relative sea-level change.

#### 4.7. Bouar–Tabarja area

An elevated shoreline is seen almost continuously from south of Nahr Ibrahim to the northern border of Jounié Bay. The evidence mainly comprises a bench a few decimetres high, cut into the Turonian limestone, and often ending landward with a palaeo-tidal notch. This elevated bench surface is currently dissected by weathering and marine erosion. We were, however, able to observe and sample marine organisms in growth position, attached to the bench surface or at the notch base. It is important to note that, generally, this elevated platform is twice to three times more developed than the

present one (Sanlaville, 1977). The platform is narrow along the sheltered micro-creeks and larger in more exposed sectors.

South of the Nahr Ibrahim estuary, a vermetid sample (LIB 2001-10) collected at the base of the +60 cm midlittoral notch was dated  $2065 \pm 40$  BP. North of Bouar creek, a small man-made basin has been cut into the limestone. It possibly corresponds to an ancient funerary chamber later used as a fish tank, with a channel opening to the sea. The channel leads to a bench at ca. +80 cm. Barnacle shells, collected in living position from a channel wall (LIB 2000-11 at 80 cm), were dated  $1160 \pm 30$  BP.

In a small creek north of Bouar, a marine algal crust partially composed of *N. notarisii*, lies at the base of a midlittoral notch (ca. +80 cm). The sample (LIB 2000-17) yielded an age of  $3195 \pm 35$  BP. Near Safra, at



La Petite Fontaine beach (Fig. 6), a *Dendropoma* sample (LIB 2000-3) collected at ca. +60 cm, yielded an age of  $1960 \pm 35$  BP. Also in Safra, north of the Rabiya Marine Royal, another *Dendropoma* sample (ca. +80 cm) from the base of an elevated midlittoral notch (LIB 2000-8), was dated  $1975 \pm 45$  BP.

In the same geomorphic context, dates for the so-called “Tabarjan” shoreline are derived from two vermetid samples collected near Tabarja (MC-63 at  $2035 \pm 13$  BP and MC-64 at  $1960 \pm 40$  BP) (Sanlaville et al., 1997). In the same area, a *Dendropoma* sample (LIB 2000-7), collected at ca. +60 cm from the surface of the elevated bench, yielded an age of  $1970 \pm 35$  BP, consistent with previous dates. A second *Dendropoma* sample (LIB 2000-4) collected at +80 cm, just a few metres from the previous one, yielded a younger age ( $1585 \pm 35$  BP), whilst an algal crust (LIB 2000-6) collected at +50 cm gave a slightly older date ( $2220 \pm 35$  BP) (Fig. 7). A few metres to the south, a well-preserved *Dendropoma* sample (LIB 2001-8) yielded an age of  $1805 \pm 30$  BP at +120 cm.

#### 4.8. Saida area

South of Beirut, elevated shoreline markers are more scattered and their elevation is generally lower. On Zire island, just offshore from Saida, the bottom of an ancient quarry (Fig. 8) is sealed by a beach-rock at ca. +50 cm containing quarried blocks mixed with well-preserved shells of *Pirenella conica*. The radiocarbon age of these shells (LIB 2001-27) constrains the submergence of the quarry to  $2210 \pm 50$  BP. The margins of the quarry also show an uplifted notch at +50 cm concomitant with this drowning phase. Close examination of beach-rock specimens in thin sections shows a sediment dominated by sand-sized pieces of branched coralline algae, mixed with debris of molluscs and siliceous particles (Fig. 8B and C). The rock is of grain-stone texture, changing laterally into wackestone. The intergranular pores are partially to totally infilled by two distinct generations of cements. The earlier precipitated cement fabric was pore-rounding, with calcite granular fringes. It is

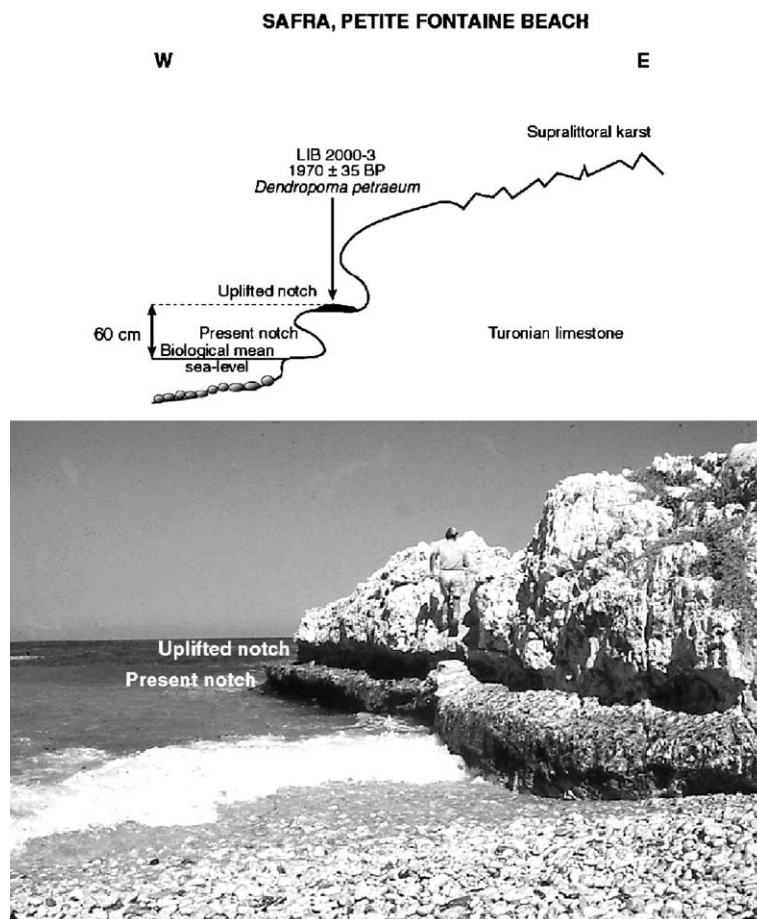


Fig. 6. Schematic section of the sample LIB 2000-3 collected in Safra La Petite Fontaine beach and corresponding photograph.

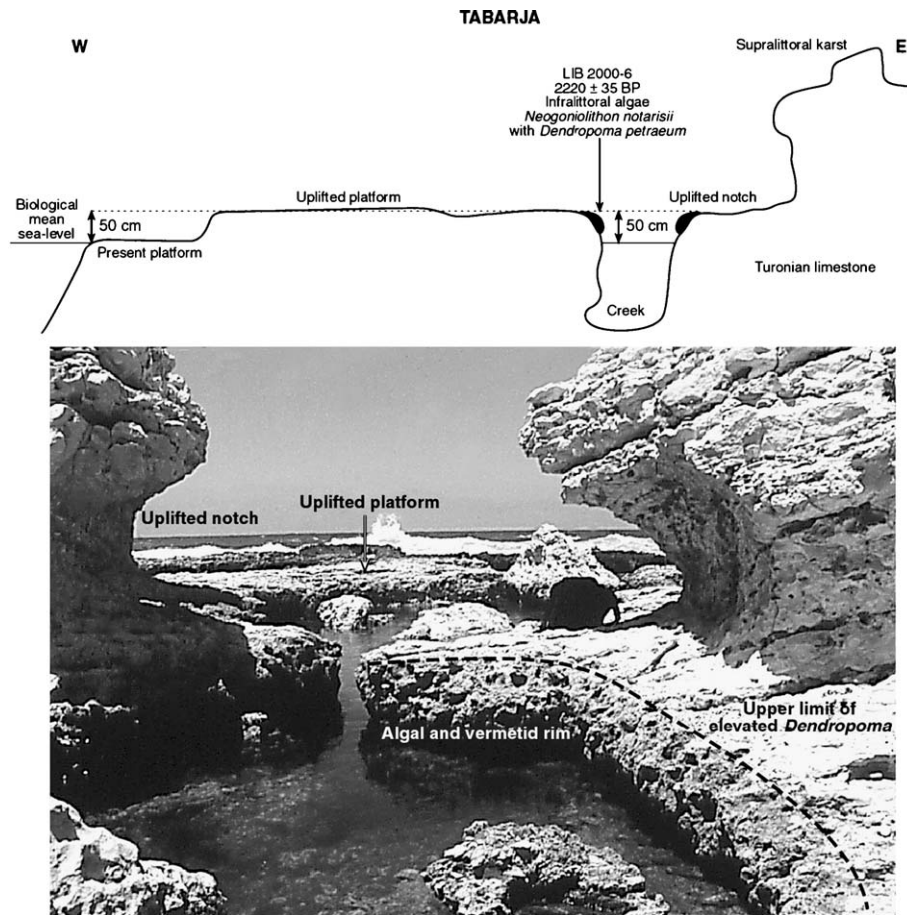


Fig. 7. Schematic section of the sample LIB 2000-6 collected in the Tabarja area and corresponding photograph.

clearly of meteoric origin. The later cementation stage has yielded a structureless, micrite matrix that has embedded marine detritus and occupied the residual pore spaces. It is obvious that this sediment has experienced at least two different diagenetic environments, meteoric followed by marine (Coudray and Montaggioni, 1986). The depositional and diagenetic history of the beach could have been as follows: 1) deposition of sand-grained sediments along the shore; 2) relative sea-level drop promoting the precipitation of meteoric cements within the sand pores; 3) relative sea-level rise, accompanied by the precipitation of marine micrites that have occluded residual porosity; 4) final emergence of the beach-rock deposit. Zire island has therefore undergone a minor ‘yo-yo’ movement, with just the onset of the downward tendency being dated.

Fifteen kilometres south of Saida, near Ras Qantara, a sample of *Vermetus triqueter* (LIB 2000-1), collected in growth position on a midlittoral platform at ca. +50 cm, yielded an age of  $2230 \pm 35$  BP.

#### 4.9. Ras Abou Zeid

Between Minet Abou Zebel and Ras Minet Abou Zeid (Aadloun sector), an elevated midlittoral notch at +70 cm above the present abrasion platform indicates a former sea-level position (Fig. 9). A *V. triqueter* sample (LIB 2000-2) at this same elevation was dated  $2525 \pm 35$  BP near marks of *Lithophaga* holes. This outcrop is sealed by beach-rock, and its age therefore corresponds to the death of the vermetids by sand accumulation before any relative sea-level change took place.

#### 4.10. Khaizerane area

South of Hotel Mounes, the Khaizerane coastal area is characterised by patchy *Dendropoma* bioconstructions overlying a beach-rock at +40 cm. These bioconstructions (LIB 2002-19) yielded a radiocarbon age of  $1095 \pm 30$  BP. This young age may be correlated with the elevated barnacles dated at Bouar (see Discussion below).

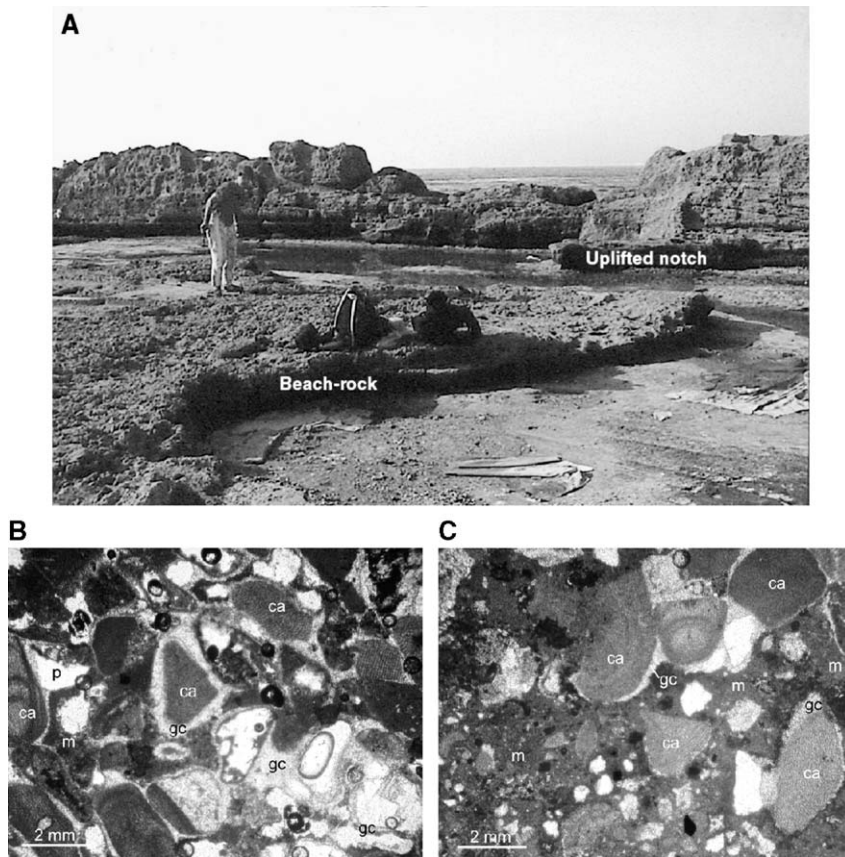


Fig. 8. A: Beach-rock at +50 cm in Zire island (Saida). B and C: Thin sections of sample LIB 2001-27. The diagenetic sequences show the occurrence of an earlier meteoric cement precipitated in the form of granular calcitic, pore-rounding fringes to mosaics (gc), followed by the deposition of a marine micrite matrix (m) within residual voids. ca = coralline algal clasts, p = residual pores.

#### 4.11. Tyre area

Our underwater geoarchaeological surveys in Tyre uncovered a submerged quarry floor 2 m below present sea level. The quarry belongs to the so-called “southern harbour” basin. On the northern side of Tyre, the top of the submerged (Roman?) mole, which would have sheltered the ancient northern harbour, is also found 2.5 m below present sea level (Poidebard, 1939; Marriner et al., 2005; Marriner et al., 2006). A living *Dendropoma* rim (Lib 2002-20) was sampled on the outer edge of an abrasion platform at  $-5 \pm 5$  cm, in order to date the base of the present bioconstruction. Constrained to  $450 \pm 50$  BP, it marks the onset of sea-level stability in the Tyre area.

## 5. Discussion

It is critical to discuss two main issues: (1) the timing of relative sea-level changes since 6000 BP, and (2) the

spatial distribution of the former sea-level markers with respect to the tectonic pattern.

### 5.1. Timing of relative sea-level changes since 6000 BP

Fig. 10 shows two main episodes of relative sea-level variations. The first peak corresponds to an older and upper elevated shoreline (ca. 2700–2200 BP) and appears to belong to Sanlaville’s (1970) so-called “Zennadian” episode. The second peak comprises a younger shoreline (ca. 2100–1800 BP or 300–650 cal. AD) at a lower elevation. This pronounced peak is composed of 12  $^{14}\text{C}$  dates (i.e. 36% of the radiocarbon data) and appears to belong to the so-called “Tabarjan” episode (Sanlaville, 1970).

#### 5.1.1. The upper raised shoreline

Evidence for elevated beach deposits were discovered near the village of Cheikh Zennad, close to the Syrian border (Sanlaville et al., 1997). These were tentatively dated to 2000–1500 BC and ascribed to a





Fig. 9. Schematic section of the sample LIB 2000-2 collected at Ras Abou Zeid and corresponding photograph.

former elevated sea level called the “Zennadian”, the elevation of which remained uncertain. A vermetid sample collected from Ile du Palmier at +220 cm and dated  $3490 \pm 80$  BP (MC-145) may indicate the elevation of this upper raised shoreline. However, our systematic survey did not reveal any geomorphological or biological evidence for a shoreline at +220 cm on Ile du Palmier, or even elsewhere along the Lebanese coast. Instead, we identified various marks of an elevated

shoreline at ca. +120 to +140 cm. This elevated shoreline is poorly preserved, but its remains are clearly distinguished from those of the slightly lower raised shoreline.

Where marks of two elevated shorelines are identified in the same section, the uppermost level is only 20 to 40 cm higher than the lower one. For example, west of Tripoli at Ile du Phare, an age of  $5975 \pm 40$  BP was obtained for this slightly higher sea level (Fig. 3A and

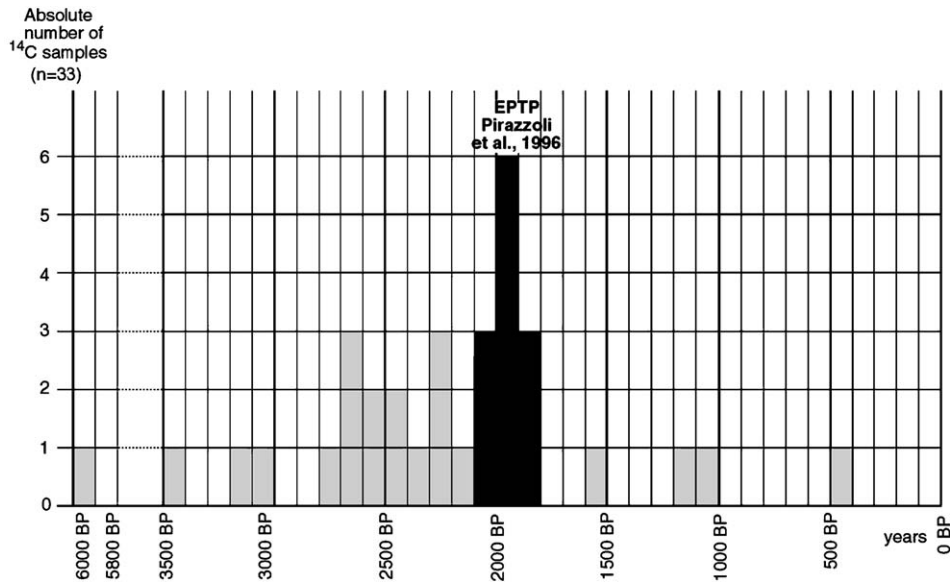


Fig. 10.  $^{14}\text{C}$  histogram of the 33 Lebanese samples.

B). Therefore, we cannot confirm an elevation of +220 cm for the so-called “Zennadian” shoreline in Lebanon. According to our data, the elevation of an upper Holocene shoreline was not more than 120–140 ( $\pm 30$ ) cm above present.

At the Eastern Mediterranean scale, a similar shoreline has been reported north of Lebanon: (a) from the Syrian coast, at between +0.7 and +2.8 m and dated ca. 2900 to 2800 BP (Dalongeville et al., 1993), and (b) at +2 m around the Orontes delta area in Turkey, uplifted around 3000 BP (Pirazzoli et al., 1991). South of Lebanon, from Israel to Gaza and the Sinai, no evidence is found for an elevated shoreline above present MSL (Galili et al., 1998; Sivan et al., 2001). This indicates that only the northern Levant coast was uplifted around 3000 BP.

#### 5.1.2. The lower raised shoreline

Along the Syrian and Lebanese coast, a +60 cm corrosion platform is very frequent. In Lebanon, this episode was dated to between ca. 1900 and 2000 BP (Sanlaville, 1977). Fig. 10 shows a peak between 2100 and 1800 BP, which correlates Sanlaville’s “Tabarjan” episode. This pattern consists of an end-peak corresponding to vermetids having developed just before the EBTP event and an irregular tail of older biological remains.

#### 5.1.3. The short Medieval episode

The younger radiocarbon ages, ca. 1100 BP (LIB 2000-11, LIB 2002-19) obtained near Bouar and north

of Tyre show evidence for an event similar to that reported from Syria (Dalongeville et al., 1993). At Ras Ibn Hani, after the 6th century AD uplift, sea level stabilised promoting the development of a *Dendropoma* rim at present sea level dated 550 to 770 AD. Some centuries later, however, evidence for relative sea-level rise is provided by marine crusts preserved at Ras el-Bassit at  $+60 \pm 20$  cm. These are constrained by six consistent radiocarbon measurements to between the 10th and the 11th centuries AD (Sanlaville et al., 1997). The two Lebanese samples from Bouar and Khaizerane seem to provide evidence for a similar rapid relative sea-level rise, of probable tectonic origin, that reached several decimetres in amplitude.

#### 5.1.4. Historical relative sea-level stabilisation

Our results constrain relative sea-level stability along the Lebanese coast to 1000 BP and later. This stability is documented by two types of indicators. The first include in situ coastal archaeological remains located at present sea level, such as fish tanks and sea walls. Along the Israeli coast, similar remains testify to a general sea-level stabilisation during historical times (Raban and Galili, 1985; Galili et al., 1988; Galili and Sharvit, 1998; Sivan et al., 2001). In Lebanon, this evolution explains the important development of present midlittoral abrasion platforms and the bioconstruction of large *Dendropoma* rims. Radiometric dating (in progress) of the contact between the base of these bioconstructions and the substratum, consistently shows dates younger than 1000 BP along the Lebanese and Israeli coasts. This

relative stability suggests the block, bounded to the east by the Dead Sea and Roum faults and containing the Carmel fault, remained stationary throughout this period.

### 5.2. RSL changes vs. crustal mobility

At a regional scale, the fact that the lower raised shoreline is found almost along the entire Lebanese coast suggests its distribution may be related to uplift of a large tectonic domain driven by slip along the Yammuneh fault (Fig. 2). Nevertheless, our data question the role of the RTT. The majority of the evidence for uplifted shorelines around 2100–1800 BP is located east of the inferred offshore trace of the RTT. Therefore, it appears that the NNW trending extension of the Roum fault, which essentially marks the southern boundary of the EBTP shorelines, is consistent with coastal uplift caused by slip on the RTT. In conclusion, our data provide compelling evidence for the key role of the RTT in late Holocene tectonic uplift of the northern and central Lebanese coasts.

At a local scale, the fact that the lower raised shoreline off Tripoli is found at a higher elevation than further south, in the Jaouz fault area, precludes differential uplifts having taken place during or after the EBTP along the RTT. Uplift decreases in intensity in the Beirut area — although it is important to stress that the coast is completely urbanized — increasing again in the Saida sector, where uplift remains nonetheless lower than in northern Lebanon. Our results suggest tilting of fault-bound panels and/or differential vertical movements to have taken place across Jaouz, Madfoun, Jounié and the ENE trending faults in the vicinity of Tyre (Fig. 2). Given the geodynamic boundary conditions along the Dead Sea transform (Klinger et al., 2000), these dextral strike-slip faults are expected to show a transpressive component of slip that would be compatible with vertical offsets and tilt of the palaeo-shorelines. In conclusion, poor spatial resolution and too few samples make it difficult to show discrete changes in uplift from one sub-block of Mt. Lebanon to the other. The local amount of uplift at each site appears to vary with (a) spatial distribution of slip vector on the fault plain; (b) distance from the site to the fault plain; and (c) local inhomogeneities of surface deformation. The role of the Lebanese transverse faults therefore remains an open debate pending better spatial resolution of the uplift pattern.

### 5.3. One earthquake or several?

It is difficult to ascertain whether uplift of the lower shoreline resulted from a single seismic event or from

several large earthquakes between the 4th century AD to the mid-7th century AD (Stiros, 2001). The Levantine coast does, however, seem to have been particularly affected by the 551 AD earthquake (Plassard, 1968; Russel, 1985), suggesting a debatable unique seismic origin for each of the raised shorelines. For instance, the differential finite uplift documented by the lower shoreline (Fig. 2) calls into question the hypothesis of a single coseismic event. On the one hand, the lower shoreline episode corresponds to an age cluster of radiocarbon dates which evokes a relatively short period of intense seismic activity. Conversely, given the overall extent and diversity of the uplifts, more than 500 km coastwise, it is difficult to invoke a single-earthquake EBTP scenario. The question remains open to debate.

### 5.4. Regional comparison

Our field data clearly indicate that the southern limit of elevated late Holocene shorelines along the Levant coast coincides with the trace of the Rosh Hanikra/Ras Nakoura fault (Fig. 1) that bounds two domains (the Tyre–Saida block to the north and Galilee to the south) with contrasted relative sea-level patterns. This suggests that the Rosh Hanikra/Ras Nakoura fault was activated during seismotectonic episodes. South of that fault, relative sea-level stability during historical times suggests that the block bounded to the east by the Dead Sea fault and to the north by the Rosh Hanikra/Ras Nakoura fault and containing the Carmel fault, remained stationary during this period. In contrast, RSL and archaeological data from Tyre manifest ca. 3 m of tectonic collapse since Roman times (Marriner et al., 2006). Therefore the Galilee crustal block could be interpreted as a fixed boundary condition to the Levantine restraining bend at a time intense seismic activity and tectonic movements were taking place along the Yammuneh fault, the RTT and second-order transverse faults.

## 6. Conclusions

The Lebanese coast provides evidence for two main elevated Holocene sea levels: (1) an upper shoreline at ca. +1.2 to +1.4 m, which lasted from ca. 6000 to 3000 BP. On the nearby coasts of Syria and Turkey, this upper shoreline suggests the occurrence of seismotectonic displacement(s) around 3000 BP, decreasing in amplitude from Turkey to southern Lebanon; (2), a lower shoreline at  $+0.8 \pm 0.4$  m, developed between 2700 BP and the 6th century AD, at the time of the EBTP. These uplifted shoreline remains result from the



activation of the Yammuneh and the RTT, as well as slip along transverse faults. The Rosh Hanikra/Ras Nakoura fault marks the southern boundary of the Levantine vertical displacements, with no evidence for coastal uplift being reported from Israel during the Holocene.

## Acknowledgements

This research was financially supported by the Franco-Lebanese CEDRE program no. F60/L58. The authors warmly thank Dr. M. Beydoun, the mayors of Byblos and Tyre, the DGA (Beirut), IFAPO (Beirut), the IUF (Paris) and the Leverhulme Trust (London) for financial and technical support. The constructive suggestions of F. Antonioli, D. Chardon, K. Lambeck and D. Sivan are gratefully acknowledged. The present paper is a contribution to IGCP project 437 (Coastal environmental change during sea-level highstands).

## References

- Barash, A., Zenziper, Z., 1985. Structural and biological adaptations of Vermetidae (Gastropoda). *Boll. Malacol.* 21 (7–9), 145–176.
- Beydoun, Z.R., 1977. The Levantine countries: the geology of Syria and Lebanon (maritime regions). In: Nairn, A.E.M., Kanes, W.H., Stehli, F.G. (Eds.), *The Ocean Basins and Margins. The Eastern Mediterranean*, vol. 4a. Plenum Press, New-York, pp. 319–353.
- Butler, R.W.H., Spencer, S., Griffiths, H.M., 1998. The structural response to evolving plate kinematics during transpression: evolution of the Lebanese restraining bend of the Dead Sea Transform. In: Holdsworth, R.E., Strachan, R.A., Dewey, J.F. (Eds.), *Continental Transpressional and Transtensional Tectonics*. Geological Society, London, Special Publications, vol. 135, pp. 81–106.
- Coudray, J., Montaggioni, L.F., 1986. The diagenetic products of marine carbonates as sea-level indicators. In: Van de Plassche, O. (Ed.), *Sea-level Research: a Manual for the Collection and Evaluation of Data*. Geo Books, Norwich, pp. 311–360.
- Dalongeville, R., Laborel, J., Pirazzoli, P.A., Sanlaville, P., Arnold, M., Bernier, P., Evin, J., Montaggioni, L.F., 1993. Les variations récentes de la ligne de rivage sur le littoral syrien. *Quaternaire* 4, 45–53.
- Daëron, M., Benedetti, L., Tapponnier, P., Surssock, A., Finkel, R.C., 2004. Constraints on the post ~25 ka slip rate of the Yammouneh fault (Lebanon) using in situ cosmogenic <sup>36</sup>Cl dating of offset limestone-clast fans. *Earth Planet. Sci. Lett.* 227, 105–119.
- Daëron, M., Klinger, Y., Tapponnier, P., Elias, A., Jacques, E., Surssock, A., 2005. Sources of the large A.D. 1202 and 1759 Near East earthquakes. *Geology* 33, 529–532.
- Di Vita, A., 1990. *L'Afrique dans l'Occident Romain*. Collection Ecole Française de Rome, vol. 134, pp. 425–494.
- Dubertret, L., 1955. Carte géologique du Liban au 1:200.000, Beyrouth.
- Dubertret, L., 1975. Introduction à la carte géologique du Liban au 1:50.000. *Notes Mém. Moyen-Orient*, 13, 345–403.
- Elias, A., Tapponnier, P., Jacques, E., Daëron, M., Klinger, Y., Surssock, A., 2003. Quaternary deformation associated with the Tripoli-Roum thrust, and the rise of the Lebanese coast, AGU-EUG-EGS joint assembly. Nice 10137.
- Fevret, M., Sanlaville, P., 1965. Contribution à l'étude du littoral libanais. *Méditerranée* 6, 113–134.
- Fevret, M., Sanlaville, P., 1966. L'utilisation des vermetes dans la détermination des anciens niveaux marins. *Méditerranée* 7, 357–364.
- Galili, E., Sharvit, J., 1998. Ancient coastal installations and the tectonic stability of the Israeli coast in historical times. In: Stewart, I.S., Vita-Finzi, C. (Eds.), *Coastal Tectonics*. Geological Society, Special Publications, London, vol. 146, pp. 147–163.
- Galili, E., Weinstein-Evron, M., Ronen, A., 1988. Holocene sea-level changes based on submerged archeological sites off the Northern Carmel coast in Israel. *Quat. Res.* 29, 36–42.
- Garfunkel, Z., 1981. Internal structure of the Dead Sea leaky transform (rift) in relation to plate kinematics. *Tectonophysics* 80, 81–108.
- Gomez, F., Meghraoui, M., Darkal, A.N., Hijazi, F., Mouty, M., Suleiman, Y., Sbeinati, R., Darawcheh, R., Al-Ghazzi, R., Barazangi, M., 2003. Holocene faulting and earthquake recurrence along the Serghaya branch of the Dead Sea fault system in Syria and Lebanon. *Geophys. J. Int.* 153, 658–674.
- Guidoboni, E., Comastri, A., Traina, G., 1994. *Catalogue of Ancient Earthquakes in the Mediterranean Area Up to the 10th Century*. Istituto Nazionale di Geofisica, Roma, p. 504.
- Kallner-Amiran, D.H., 1950. A revised earthquake-catalogue of Palestine. *Isr. Explor. J.* 223–246.
- Khair, K., 2001. Geomorphology and seismicity of the Roum fault as one of the active branches of the Dead Sea fault system in Lebanon. *J. Geophys. Res.* 106, 4233–4245.
- Klinger, Y., Avouac, J.-P., Abou Karaki, N.A., Dorbath, L., Bourlès, D., Reyss, J.-L., 2000. Slip rate on the Dead Sea transform fault in northern Araba valley (Jordan). *Geophys. J. Int.* 142, 755–768.
- Laborel, J., Laborel-Deguen, F., 1994. Biological indicators of relative sea-level variations and of co-seismic displacements in the Mediterranean region. *J. Coast. Res.* 10 (2), 395–415.
- Lipkin, Y., Safriel, U., 1971. Intertidal zonation on rocky shores at Mikmoret. *J. Ecol.* 59, 1–30.
- Marriner, N., Morhange, C., Boudagher-Fadel, M., Bourcier, M., Carbonel, P., 2005. Geoarchaeology of Tyre's ancient northern harbour, Phoenicia. *J. Archaeol. Sci.* 32, 1302–1327.
- Marriner, N., Morhange, C., Doumet-Serhal, C., Carbonel, P., 2006. Geoscience rediscovers Phoenicia's buried harbors. *Geology* 34.
- Mart, Y., Perelman, I., 1996. Neotectonic activity in Caesarea, the Mediterranean coast of central Israel. *Tectonophysics* 1–2, 139–153.
- Meghraoui, M., Gomez, F., Sbeinati, R., Van der Woerd, J., Mouty, M., Darkal, A.N., Radwan, Y., Layyous, I., Al Najjar, H., Darawcheh, R., Hijazi, F., Al-Ghazzi, R., Barazangi, M., 2003. Evidence for 830 years of seismic quiescence from palaeoseismology, archaeoseismology and historical seismicity along the Dead Sea fault in Syria. *Earth Planet. Sci. Lett.* 210, 35–52.
- Poidebard, A., 1939. *Un grand port disparu: Tyr, recherches aériennes et sous-marines 1934–1936*. Librairie Orientaliste Paul Geuthner, Paris, p. 78.
- Pirazzoli, P.A., 1976. Les variations du niveau marin depuis 2000 ans. *Mémoire du Laboratoire de Géomorphologie de l'Ecole Pratique des Hautes Etudes*, vol. 30, p. 421.
- Pirazzoli, P.A., 1986a. The early Byzantine tectonic paroxysm. *Z. Geomorphol., Suppl.* 62, 31–49.
- Pirazzoli, P.A., 1986b. Marine notches. In: Van de Plassche, O. (Ed.), *Sea-Level Research: A Manual for the Collection and Evaluation of Data*. GeoBooks, Norwich, pp. 361–400.

- Pirazzoli, P.A., Laborel, J., Saliège, J.F., Erol, O., Kayan, I., Person, A., 1991. Holocene raised shorelines on the Hatay coasts (Turkey): paleoecological and tectonic implications. *Mar. Geol.* 96, 295–311.
- Pirazzoli, P.A., Stiros, S.C., Laborel, J., Laborel-Deguen, F., Arnold, M., Papageorgiou, S., Morhange, C., 1994a. Late Holocene shoreline changes related to palaeoseismic events in the Ionian Islands (Greece). *Holocene* 4, 397–405.
- Pirazzoli, P.A., Stiros, S.C., Arnold, M., Laborel, J., Laborel-Deguen, F., Papageorgiou, S., 1994b. Episodic uplift deduced from Holocene shorelines in the Perachora Peninsula (Corinth area, Greece). *Tectonophysics* 229, 201–209.
- Pirazzoli, P.A., Laborel, J., Stiros, S.C., 1996. Earthquake clustering in the Eastern Mediterranean during historical times. *J. Geophys. Res.* 101 (B3), 6083–6097.
- Plassard, J., 1968. Crise séismique au Liban du IV<sup>e</sup> au VI<sup>e</sup> siècle. *Mél. Univ. St-Joseph* 44 (2), 10–20.
- Plassard, J., Kogoj, B., 1981. Catalogue des seismes ressentis au Liban. *Ann. Sism. Observ. Ksara. CNRS, Beyrouth*, p. 47.
- Raban, A., Galili, E., 1985. Recent maritime archaeological research in Israel, a preliminary report. *Int. J. Naut. Archaeol.* 14 (4), 321–356.
- Ron, H., Eyal, Y., 1985. Intraplate deformation by block rotation and mesostructures along the Dead Sea transform, northern Israel. *Tectonics* 4, 85–105.
- Ron, H., Freund, R., Garfunkel, Z., 1984. Block rotation by strike-slip faulting: structural and paleomagnetic evidence. *J. Geophys. Res.* 89, 6256–6270.
- Russel, K.W., 1985. The earthquake chronology of Palestine and Northwest Arabia from the 2nd through the mid-8th century. *Bull. Am. School Orient. Res.* 260, 37–59.
- Safriel, U.N., 1975. The role of vermetid gastropods in the formation of Mediterranean and Atlantic reefs. *Oecologia* 20, 85–101.
- Sanlaville, P., 1970. Les variations holocènes du niveau de la mer au Liban. *Rev. Géogr. Lyon* 45 (3), 279–304.
- Sanlaville, P., 1977. Etude géomorphologique de la région littorale du Liban. *Publ. Univ. Liban., Sect. Études Géogr., Beirut* 3.
- Sanlaville, P., Dalongeville, R., Bernier, P., Evin, J., 1997. The Syrian coast: a model of Holocene coastal evolution. *J. Coast. Res.* 13 (2), 385–396.
- Sivan, D., Wdowski, S., Lambeck, K., Galili, E., Raban, A., 2001. Holocene sea-level changes along the Mediterranean coast of Israel, based on archaeological observations and numerical model. *Palaeogeogr. Palaeoclimatol. Palaeoecol.* 167, 101–117.
- Stiros, S.C., 2001. The AD 365 Crete earthquake and possible seismic clustering during the fourth to sixth centuries in the Eastern Mediterranean: a review of historical and archaeological data. *J. Struct. Geol.* 23, 545–562.
- Stiros, S.C., Pirazzoli, P.A., 1998. Late Quaternary coastal changes in the Gulf of Corinth, Greece, Geodesy Laboratory. Dept. of Civil Engineering, Patras University, Patras, p. 49.
- Stiros, S.C., Laborel, J., Laborel-Deguen, F., Papageorgiou, S., Evin, J., Pirazzoli, P.A., 2000. Seismic coastal uplift in a region of subsidence: Holocene raised shorelines of Samos Island, Aegean Sea, Greece. *Mar. Geol.* 170, 41–58.
- Stuiver, M., Reimer, P.J., Bard, E., Beck, J.W., Burr, G.S., Hughen, K. A., Kromer, B., McCormac, G., Van der Plicht, J., Spurk, M., 1998a. Intcal98 radiocarbon age calibration, 24,000–0 cal BP. *Radiocarbon* 40 (3), 1041–1083.
- Stuiver, M., Reimer, P., Braziunas, T.F., 1998b. High precision radiocarbon age calibration for terrestrial and marine samples. *Radiocarbon* 40 (3), 1127–1151.
- Tzur, Y., Safriel, U.N., 1978. Vermetid platform as indicators of coastal movements, Israel. *J. Earth-Sci.* 27, 124–127.
- Walley, C.D., 1988. A braided strike-slip model for the northern continuation of the Dead Sea fault and its implications for Levantine tectonics. *Tectonophysics* 145, 63–72.
- Walley, C.D., 1998. Some outstanding issues in the geology of Lebanon and their importance in the tectonic evolution of the Levantine region. *Tectonophysics* 298, 37–62.
- Zilberman, E., Amit, R., Heimann, A., Porat, N., 2000. Changes in paleoseismic activity in the Hula pull-apart basin, Dead Sea rift, northern Israel. *Tectonophysics* 321, 237–252.